



HAL
open science

The variety of phenotypes behind ‘double outlet right ventricle’: clinical and imaging presentations in four dogs and a cat

Valérie Chetboul, M. Roche-Catholy, A. Pun-García, P. Passavin, A. Morlet, C. Misbach, E. Trehou-Sechi, C. Poissonnier, N. Borenstein, Vittorio V. Saponaro

► To cite this version:

Valérie Chetboul, M. Roche-Catholy, A. Pun-García, P. Passavin, A. Morlet, et al.. The variety of phenotypes behind ‘double outlet right ventricle’: clinical and imaging presentations in four dogs and a cat. *Journal of Veterinary Cardiology*, 2020, 31, pp.51 - 60. 10.1016/j.jvc.2020.08.005 . hal-03492483

HAL Id: hal-03492483

<https://hal.science/hal-03492483>

Submitted on 26 Sep 2022

HAL is a multi-disciplinary open access archive for the deposit and dissemination of scientific research documents, whether they are published or not. The documents may come from teaching and research institutions in France or abroad, or from public or private research centers.

L’archive ouverte pluridisciplinaire **HAL**, est destinée au dépôt et à la diffusion de documents scientifiques de niveau recherche, publiés ou non, émanant des établissements d’enseignement et de recherche français ou étrangers, des laboratoires publics ou privés.



Distributed under a Creative Commons Attribution - NonCommercial 4.0 International License

1 **The variety of phenotypes behind “double outlet right ventricle”: clinical and**
2 **imaging presentations in four dogs and a cat**

3
4 Valérie Chetboul, DVM, PhD^{a,b}; Marine Roche-Catholy, DVM^a; Andrés Pun-García,
5 DVM, PhD^a; Peggy Passavin, DVM^a; Alexis Morlet, DVM, PhD^c; Charlotte Misbach,
6 DVM, PhD^c; Emilie Trehieu-Sechi, DVM^a; Camille Poissonnier, DVM^a; Nicolas
7 Borenstein DVM, PhD^c; Vittorio Saponaro, DVM, PhD^a

8
9 ^a Unité de Cardiologie d’Alfort (UCA), Université Paris-Est, École Nationale
10 Vétérinaire d’Alfort, Centre Hospitalier Universitaire Vétérinaire d’Alfort (CHUVA), 7
11 avenue du général de Gaulle, Maisons-Alfort, F-94700, France;

12 ^b U955 - IMRB Inserm, École Nationale Vétérinaire d’Alfort, UPEC, 7 avenue du
13 général de Gaulle, Maisons-Alfort, F-94700, France;

14 ^c IMMR, Paris, France, 42 Boulevard Jourdan, 74014 Paris, France.

15
16 Corresponding author: Prof. Valérie Chetboul (valerie.chetboul@vet-alfort.fr).

17
18 **Short title**

19 Double outlet right ventricle in small animals

20
21 This study was not supported by any grant or other funding.

22
23
24

25 **Acknowledgements**: We sincerely acknowledge the “Fondation Un Coeur”
26 (Foundation under the aegis of the “Fondation de France”), as well as the Zoetis and
27 Vetoquinol companies for having sponsored the research assistant positions of Dr.
28 Marine Roche Catholy, Dr. Camille Poissonnier and Dr. Andrés Pun-García *via* the
29 foundation at the Alfort Cardiology Unit (UCA). We also thank Dr. Cécile Damoiseaux
30 and Vassiliki Gouni as well as the Anatomical Pathology department (Dr. Edouard
31 Reyes Gomez) of the Alfort National Veterinary School.

32 **Abstract**

33 This report describes five cases of double outlet right ventricle (DORV) in four dogs
34 (3 to 18 months old; two males and two females) and a domestic shorthair cat (6-
35 month-old, female) presented with various clinical signs including tachypnea (n=5),
36 exercise intolerance (n=5), mucous cyanosis (n=3), delayed growth (n=2) and/or
37 lethargy (n=2). The represented canine breeds were Poodle, Yorkshire Terrier,
38 Samoyed, and Shetland Sheepdog.

39 For all animals, echocardiography revealed marked aortic dextroposition with both
40 arterial trunks totally arising from the right ventricle, associated with a ventricular
41 septal defect (VSD) and various other congenital abnormalities, including subvalvular
42 aortic stenosis (n=2), minor aortic insufficiency (n=5), subvalvular pulmonic stenosis
43 with pulmonary trunk hypoplasia (n=1), patent ductus arteriosus (n=1), minor mitral
44 and/or tricuspid dysplasia (n=3). Subsequent cardiac remodeling was characterized
45 by marked right ventricular hypertrophy for all patients, associated with right
46 ventricular and right atrial dilation for most of them (4/5).

47 Two dogs died soon after the initial DORV diagnosis (i.e., after 24 hours and two
48 months). A surgical correction attempted for another dog confirmed the presence of a
49 DORV associated with patent ductus arteriosus, but the animal died during the
50 procedure from sudden cardiac arrest. The fourth dog underwent a contrast-
51 enhanced retrospective electrocardiogram-gated multidetector computed tomography
52 angiography under general anesthesia, which confirmed the conotruncal
53 malformation. Despite episodes of exercise intolerance, this dog is still alive, at the
54 age of 48 months, as is the cat at the age of 16 months.

55

56 **Key words:** Canine; Congenital; Doppler; Feline; Heart

57 **Abbreviations**

bpm	beats per minute
CT	computed tomography
DORV	double outlet right ventricle
ECG	electrocardiographic
LV	left ventricle
LVPWs	left ventricular posterior wall thickness at end-systole
PCV	packed cell volume
RA	right atrium
RBC	red blood cells
RV	right ventricle
RVFWs	right ventricular free wall at end-systole
RVDd	right ventricular dimension at end-diastole
TGA	transposition of the great arteries
VSD	ventricular septal defect

58

59 **Case 1**

60 A 17-month-old male Poodle dog, weighing 5.0 kg, was referred to the Alfort
61 Cardiology Unit (UCA) at the Veterinary Hospital (CHUVA) of the Alfort National
62 Veterinary School (ENVA) for exercise intolerance and intermittent tachypnea, which
63 had both worsened over the past three months. The physical examination showed
64 congested mucous membranes and a grade I/VI right basilar systolic heart murmur.
65 Two- and three-dimensional echocardiographic examination^d coupled with color- and
66 continuous-wave Doppler modes (Figs. 1A and 1B), revealed a large doubly
67 committed ventricular septal defect (VSD; maximal diameter: 16 mm) characterized
68 by an intermittent bilateral low-velocity shunt (left-to-right in systole and right-to-left in
69 early-diastole, with a maximal velocity of 1.1 and 0.9 m/s respectively, and absent at
70 end-diastole). Severe aorta dextroposition was also observed, with the aorta entirely
71 originating from the right ventricle. Minor aortic insufficiency was also noted. Based
72 on these echocardiographic findings, the dog was diagnosed with double outlet right
73 ventricle (DORV). The peak systolic transpulmonary flow velocity assessed using
74 continuous-wave Doppler mode was 2.0 m/s. End-systolic right ventricular free wall
75 and left ventricular posterior wall thicknesses (RVFWs and LVPWs, respectively)
76 were measured using the two-dimensional guided M-mode from the right parasternal
77 ventricular short-axis view, and confirmed marked right ventricular (RV) wall
78 thickening (RVFWs:LVPWs ratio = 130%, reference interval: 24-50%, [1]), associated
79 with RV dilation (RV end-diastolic diameter (RVDd) to left ventricular end-diastolic
80 diameter ratio of 79%, reference interval: 7-33% [1]), and a paradoxical septal
81 motion. The right atrium (RA) was also markedly dilated, with a right to left atrium
82 ratio (measured at end-diastole at the level of the atrioventricular valves using the
83 right parasternal 4-chamber view) of 1.4 (reference range: 0.6-1.0 [2]). The caudal

84 vena cava was unremarkable. Minor mitral and tricuspid insufficiencies, associated
85 with mild leaflet remodeling, were also observed. Concomitant electrocardiographic
86 (ECG) tracing showed a normal sinus rhythm with right axis deviation (heart rate
87 between 80 and 100 beats per minute (bpm)).

88 To better describe the cardiac and vessels malformations, a contrast-enhanced
89 multidetector computed tomography (CT) angiography with retrospective ECG-gated
90 reconstructions^{e,f} was subsequently performed under general anesthesia (Figs. 1C
91 and 1D; Videos 1 to 3). This confirmed the association of severe aortic dextroposition
92 and a large doubly committed VSD, with secondary marked RA and RV dilation
93 associated with RV hypertrophy. A subpulmonary infundibulum was observed without
94 any subaortic infundibulum. An aberrant coronary artery emerging from the
95 pulmonary trunk was also detected (Fig. 1D). Hematology revealed mild
96 polycythemia (red blood cells (RBC) = $8.9 \times 10^{12}/L$, reference range: $5.5-8.5 \times 10^{12}/L$;
97 hemoglobin = 21.3 g/dL, reference range: 10.0-18.0 g/L; packed cell volume (PCV) =
98 55.2%, reference range: 35.0-55.0%). Biochemistry was unremarkable.

99 An oral medical treatment (spironolactone^g 0.5 mg/kg/day and omega-3 fatty acids^h)
100 was prescribed. At the time of writing, this dog is still alive at the age of 48 months
101 and appears in good physical condition, despite some episodes of exercise
102 intolerance.

103

104 **Case 2**

105 A 1.5-year-old female Yorkshire Terrier dog, weighing 3.9 kg, was referred for
106 chronic seizures, which had intensified over the previous week. Episodes of
107 weakness, exercise intolerance and dyspnea had been reported since birth. An oral
108 medical treatment that included benazeprilⁱ 0.3 mg/kg/day and spironolactone^g 1.3

109 mg/kg/day with furosemide^j (1.3 mg/kg) in the case of dyspnea, was prescribed at 2
110 months of age by the referral veterinarian,
111 Upon admission, the animal was lethargic, cyanotic and tachypneic. Cardiac
112 auscultation revealed a grade V/VI right mediothoracic systolic heart murmur and a
113 grade IV/VI left basilar systolic heart murmur.
114 Two-dimensional and Doppler echocardiography^d led to diagnosis of a DORV
115 characterized by an aorta emerging entirely from the RV, along with a small (3.7 mm)
116 non-committed muscular VSD, causing a left-to-right shunt (peak velocity of 5.6 m/s;
117 Figs. 2A and 2B). A subpulmonary infundibulum was clearly observed without any
118 subaortic infundibulum. The pulmonic flow assessed using color-flow Doppler mode
119 was laminar. Conversely, the aortic flow was turbulent and showed an increased
120 peak velocity (5.52 m/s; peak systolic pressure gradient = 126 mmHg) due to the
121 presence of subvalvular aortic stenosis, with concomitant mild aortic insufficiency.
122 Right ventricular hypertrophy (RVFWs:LVPWs ratio = 81% [1]), along with left
123 ventricular (LV) hypertrophy and a secondary decrease of LV internal diameters,
124 were also noted (normalized LV end-diastolic and end-systolic internal diameters of
125 1.0 and 0.7 [3]). Dilation of the pulmonary trunk, associated with a “notched” Doppler
126 flow pattern of the pulmonary artery flow and decreased peak systolic
127 transpulmonary flow velocity (0.49 m/s [4,5]), suggestive of pulmonary arterial
128 hypertension, were also observed. Concomitant ECG tracing displayed a sinus
129 rhythm without any significant abnormality (heart rate between 90 and 110 bpm).
130 Complete blood count revealed severe polycythemia (RBC = $12.09 \times 10^{12}/L$ and PCV
131 = 84%). The dog died suddenly 24 hours after diagnosis.
132 The postmortem examination (Fig. 2C) confirmed the presence of all the
133 echocardiographic abnormalities (DORV, VSD and subvalvular aortic stenosis).

134 Histopathological examination of the lungs (Fig. 2D) revealed severe remodeling of
135 the pulmonary arteries, with plexiform arterial networks, hypertrophy of the media,
136 intimal fibrosis and thrombosis, all of which were consistent with chronic pulmonary
137 arterial hypertension.

138

139 **Case 3**

140 A 4-month-old male Samoyed puppy (8.1 kg) was referred for exercise intolerance,
141 lethargy, shortness of breath, mucous cyanosis, and occasional coughing, that had
142 worsened over the last two weeks.

143 On presentation, the main physical examination findings included tachypnea with
144 mild mucous cyanosis and delayed growth. Cardiac auscultation revealed a grade
145 II/VI right mediothoracic systolic murmur and a grade II/VI left basilar diastolic
146 murmur.

147 Two- and three-dimensional echocardiographic examination, coupled with color-flow
148 Doppler mode (Fig. 3A),^d revealed a DORV, with complete aorta dextroposition
149 associated with mild aortic insufficiency. A subpulmonary infundibulum was clearly
150 observed without any subaortic infundibulum. The peak systolic transpulmonary flow
151 velocity assessed using continuous-wave Doppler mode was 1.4 m/s. A large
152 perimembranous subaortic VSD (up to 1.4 cm) with bilateral low-velocity shunt
153 (mostly left-to-right: 1.69 m/s, gradient = 11 mmHg) was also observed. The RV was
154 severely hypertrophied and dilated (RVFWs:LVPWs ratio = 206%; RVDd to LV end-
155 diastolic diameter ratio = 103% [1]), leading to a paradoxical septal motion and
156 remarkably decreased LV diameters (normalized LV end-diastolic and end-systolic
157 internal diameters of 0.9 and 0.6, respectively [3]). The RA was also markedly dilated
158 (right to left atrium ratio = 1.8 [2]), with secondary dilation of the caudal vena cava.

159 The pulmonary trunk and RV outflow tract were also dilated. A high velocity
160 pulmonary insufficiency was observed (4.41 m/s at end-diastole, gradient = 78
161 mmHg), suggesting the presence of severe diastolic pulmonary arterial hypertension.
162 Additionally, using color-flow Doppler mode from the right parasternal transaortic
163 short-axis view, an ascending non-aliased low velocity flow was visualized within the
164 pulmonary trunk, consistent with a patent ductus arteriosus providing a left-to-right
165 low velocity shunt (Fig. 3B). Lastly, a mild mitral insufficiency accounting for minor
166 mitral dysplasia, was found. The concurrent electrocardiogram showed a sinus
167 rhythm with right axis deviation (heart rate between 130 and 175 bpm). The PCV was
168 54%.

169 Spironolactone⁹ (1.2 mg/kg/day per os) was initially prescribed. A surgical correction
170 under cardiopulmonary bypass was planned with the main objective to suture a patch
171 in order to isolate the connection between the aorta to the LV while leaving the
172 pulmonary trunk connected to the RV. Unfortunately, the patient died when starting
173 cardiopulmonary bypass owing to ventricular fibrillation. The view of the open heart
174 confirmed a DORV associated with a subaortic VSD and a patent ductus arteriosus.
175 A histopathological examination was declined by the owners.

176

177 **Case 4**

178 A 3-month-old female Shetland Sheepdog (5.5 kg) was referred for suspected
179 congenital heart disease. The owners reported exercise intolerance and mucous
180 cyanosis. Physical examination findings included delayed growth, mucous cyanosis,
181 tachypnea, and grade IV/VI left basilar systolic heart murmur.

182 Two-dimensional and Doppler echocardiography^d was subsequently performed and
183 revealed a DORV, with the aorta emerging completely from the RV without any well-

184 defined subaortic infundibulum. A severe subvalvular aortic stenosis was also
185 observed (trans-stenotic peak pressure gradient = 127 mmHg) with mild aortic
186 insufficiency. A small-diameter (3.1 mm) subaortic VSD, leading to a bidirectional
187 interventricular shunt, was also noted. Assessment of the pulmonary outflow tract
188 revealed pulmonary trunk hypoplasia, associated with severe infundibular pulmonary
189 stenosis (peak systolic transpulmonary flow velocity assessed using continuous-
190 wave Doppler mode = 6.4 m/s; trans-stenotic peak pressure gradient = 165 mmHg).
191 Consequently, the RV was severely hypertrophied and dilated (RVFWs:LVPWs ratio
192 = 169%; RVDd to LV end-diastolic diameter ratio = 89% [1]), as was the RA (right to
193 left atrium ratio = 1.4 [2]). Hypertrophy of the interventricular septum was also
194 observed, as well as decreased LV internal diameters (normalized LV end-diastolic
195 and end-systolic internal diameters of 0.8 and 0.3, respectively [3]). Minor mitral
196 insufficiency resulting from mild leaflet remodeling was also found. The concomitant
197 electrocardiogram showed a respiratory sinus arrhythmia (heart rate between 90 and
198 120 bpm). Hematology confirmed polycythemia (RBC = $9.82 \times 10^{12}/L$; PCV = 74%).
199 No medication was prescribed according to the owner's request. The animal died
200 suddenly at home two months after the initial diagnosis, and no necropsy could be
201 performed.

202

203 **Case 5**

204 A 6-month-old 2.5 kg domestic shorthair female cat was referred for exercise
205 intolerance and episodic dyspnea. The cat exhibited tachypnea after minimal manual
206 restraint, and auscultation revealed a grade IV/VI right mediothoracic systolic heart
207 murmur.

208 Transthoracic echocardiography was subsequently performed,^d and confirmed that
209 the aorta emerged entirely from the RV and was even located on the right side of the
210 pulmonary trunk (Figs. 4A and B). A short bilateral infundibulum emerging from the
211 RV was seen. A large muscular VSD (Fig. 4C) mainly committed with the pulmonary
212 trunk was also found, so that the LV ejection flow passed through the VSD towards
213 both arteries, but mostly into the pulmonary trunk. A mild aortic insufficiency was
214 detected. The peak systolic transpulmonary flow velocity assessed using continuous-
215 was Doppler mode was 1.3 m/s. A pulmonary insufficiency of high velocity (3.14 m/s)
216 was also present suggesting diastolic pulmonary arterial hypertension. Accordingly,
217 the RV was both hypertrophied and dilated, with a mild RA dilation. The
218 interventricular flow was mostly left-to-right and was characterized by a low peak
219 velocity (1.2 m/s), indicating a very low-pressure gradient (6 mmHg) owing to high
220 RV systolic pressure, and was rarely right-to-left at end systole and early diastole.
221 Concomitant ECG tracing showed a normal sinus rhythm (150 bpm) along with right
222 axis deviation. Hematology confirmed polycythemia (RBC = $9.82 \times 10^{12}/L$; PCV =
223 74%). A cardiac CT scan was proposed but the owner preferred a more conservative
224 approach and consented only to medical palliation. This consisted of spironolactone⁹
225 (1 mg/kg/day). The cat is still alive at the age of 16 months and the owners report an
226 improvement of tachypnea.

227

228

229 **Discussion**

230 Double outlet right ventricle is a congenital heart disease encompassing a wide
231 spectrum of anatomic abnormalities and pathophysiologic disturbances, explaining
232 many controversies in human cardiology regarding its definition, nomenclature, and

233 classification as well as optimal timing for surgical repair [6]. According to the
234 consensus definition issued by the *Congenital Heart Surgery Nomenclature and*
235 *Database Project*, DORV is a rare conotruncal anomaly corresponding to a particular
236 ventriculo-arterial connection, in which the two arterial trunks emerge entirely or
237 predominantly from the RV [6]. In most cases, viability is provided by the presence of
238 a VSD associated with various structural connections to both arteries and allowing
239 blood to flow from the LV to the RV, and then into the pulmonary and systemic
240 circulations. In humans, DORV only accounts for approximately 1 to 3% of congenital
241 cardiac defects [7]. Veterinary retrospective studies suggest that DORV is also a rare
242 congenital malformation in both cats and dogs, accounting for 0.5% to 1% of
243 congenital cardiac defects in cats [8,9], with no DORV cases in retrospective reviews
244 performed on 105 to 976 dogs with congenital heart diseases [8,10,11]. A few
245 isolated case reports, relying essentially on postmortem examinations, have
246 documented this condition in dogs and cats [12-15], horses [16,17], alpacas [18] and
247 calves [19,20]. To the best of our knowledge, the present report is the first case
248 series with an antemortem DORV diagnosis in small animals, i.e., four dogs and one
249 cat. In all five animals, the echocardiographic diagnosis of DORV was based on the
250 presence of a VSD associated with complete commitment of the aorta to the RV,
251 which could be confirmed by CT scan (Case 1) and by necropsy in two cases (Cases
252 2 and 3). The diagnosis of DORV in Cases 4 and 5 was solely based on
253 echocardiography, which represents a limitation of the present report.

254 The first DORV description was done in 1898, but the term “DORV” was not
255 introduced until 1957, as the defect was initially considered as a particular form of
256 transposition of the great arteries (TGA) [21]. The double outlet left ventricle, another
257 abnormal type of ventriculoarterial connection in which both great arteries arise

258 entirely or predominantly from the LV, was then described several years later [22]. In
259 humans, DORV is a complex cardiac malformation characterized by great
260 heterogeneity among affected patients, depending on the VSD characteristics, the
261 spatial relationship between the VSD and the arterial trunks and between the arterial
262 trunks themselves, and the presence or absence of pulmonic or aortic stenosis, and
263 of other concomitant malformations [6,7,23]. The VSD characteristics include its
264 restrictive or unrestrictive features and also its location, with subaortic VSD being the
265 most common type in human patients with DORV, accounting for approximately 50%
266 of surgical patients [6]. Thus, as illustrated in the present case series, DORV
267 encompasses a wide spectrum of anatomic defects, with a great variability of clinical
268 presentations and pathophysiologic features, including extreme forms mimicking
269 either tetralogy of Fallot or TGA in the case of respectively associated pulmonic
270 stenosis and subpulmonary VSD [6,23]. Various classifications of DORV taking into
271 account these anatomic variations have been proposed in an attempt to standardize
272 surgical approaches in human patients [6,23,24]. One of the most commonly used
273 DORV classification systems identifies four DORV types, i.e., the VSD type (including
274 DORV with subaortic or doubly-committed VSD and without pulmonic stenosis), the
275 tetralogy of Fallot type (including DORV with subaortic or doubly-committed VSD and
276 pulmonic stenosis), the TGA type (including DORV with subpulmonary VSD) and the
277 remote VSD type characterized by a non-committed VSD (i.e., a VSD distant from
278 the arterial trunks, observed in the muscular interventricular septum) [6]. According to
279 this classification, two DORV types were diagnosed in the present report, and
280 confirmed by either necropsy or CT scan, i.e., two VSD types for Cases 1 and 3
281 (characterized by a doubly-committed or subaortic VSD in the absence of pulmonic
282 stenosis) and one remote VSD type for Case 2. Case 4 can be classified as a

283 tetralogy of Fallot type DORV, owing to the concomitant presence of severe
284 infundibular pulmonary stenosis, and Case 5 as a TGA type owing to the
285 echocardiographic visualization of a large muscular subpulmonary VSD. However,
286 since the latter two descriptions were limited to echocardiographic examinations, the
287 exact location of the VSD, especially for Case 5, could not be confirmed with
288 certainty.

289 Beside its above-mentioned extreme anatomic variability, DORV in human patients is
290 also characterized by its common association with multiple cardiac malformations
291 [6,25]. In this context, CT scan has been shown to be an excellent diagnostic tool for
292 detecting DORV-associated malformations, and a combination of transthoracic
293 echocardiography with CT scan allows excellent diagnostic performance (100 %
294 sensitivity for detecting intracardiac anomalies *versus* 91% for echocardiography
295 alone) [25]. Only one dog in the present case series was able to benefit from these
296 combined imaging techniques (Case 1), as the other dogs were presented before
297 acquisition of the CT-scan technique in our facility, while the cat's owners declined
298 the investigation. Nevertheless, various congenital abnormalities were found
299 associated with DORV in all the animals, including subvalvular aortic stenosis (n=2),
300 aortic insufficiency (n=5), subvalvular pulmonic stenosis with pulmonary trunk
301 hypoplasia (n=1), patent ductus arteriosus (n=1), and minor atrioventricular dysplasia
302 (n=3). Understandably, the variety of both the anatomic DORV phenotypes and
303 associated malformations explains the wide range of clinical presentations, as
304 illustrated in the present report.

305

306 In conclusion, this short case series illustrates the wide spectrum of congenital
307 anatomic anomalies, associated defects, and clinical presentations embodied by

308 DORV in small animals. Echocardiography remains adequate to reach a diagnosis.
309 However, owing to the complexity and heterogeneity of DORV, a cardiac CT scan
310 appears to be a wise option before attempting any surgical approach.

311 **References**

312

313 [1] Chetboul C, Damoiseaux C, Lefebvre HP, Concordet D, Desquilbet L, Gouni
314 V, Poissonnier C, Pouchelon J-L, Tissier R. Quantitative assessment of both systolic
315 and diastolic right ventricular morphology and function by conventional
316 echocardiography and speckle tracking imaging in dogs: a prospective study in 104
317 healthy dogs. *J Vet Sci* 2018;19:683-92.

318 [2] Serres F, Chetboul V, Tissier R, Gouni V, Desmyter A, Sampedrano CC,
319 Pouchelon JL. Quantification of pulmonary to systemic flow ratio by a Doppler
320 echocardiographic method in the normal dog: Repeatability, reproducibility, and
321 reference ranges. *J Vet Cardiol* 2009;11:23-9.

322 [3] Cornell CC, Kittleson MD, Della Torre P, Häggström J, Lombard CW,
323 Pedersen HD, Vollmar A, Wey A. Allometric scaling of M-mode cardiac
324 measurements in normal adult dogs. *J Vet Intern Med* 2004;18:311-21.

325 [4] Chetboul V, Sampedrano CC, Concordet D, Tissier R, Lamour T, Ginesta J,
326 Gouni V, Nicolle AP, Pouchelon JL, Lefebvre HP. Use of quantitative two-
327 dimensional color tissue Doppler imaging for assessment of left ventricular radial and
328 longitudinal myocardial velocities in dogs. *Am J Vet Res* 2005;66:953-61.

329 [5] Serres F, Chetboul V, Gouni V, Tissier R, Sampedrano CC, Pouchelon JL.
330 Diagnostic value of echo-Doppler and tissue Doppler imaging in dogs with pulmonary
331 arterial hypertension. *J Vet Intern Med* 2007;21:1280-9.

332 [6] Walters H, Mavroudis C, Tchervenkov C, Jacobs J, Lacour-Gayet F, Jacobs
333 M. Congenital heart surgery nomenclature and database project: double outlet right
334 ventricle. *Ann Thorac Surg* 2000;69:249-63.

- 335 [7] Obler D, Juraszek AL, Smoot LB, Natowicz MR. Double outlet right ventricle:
336 aetiologies and associations. *J Med Genet* 2008;45:481-97.
- 337 [8] Schrope DP. Prevalence of congenital heart disease in 76,301 mixed-breed
338 dogs and 57,025 mixed-breed cats. *J Vet Cardiol* 2015;17:192-202.
- 339 [9] Tidholm A, Ljungvall I, Michal J, Häggström J, Höglund K. Congenital heart
340 defects in cats: A retrospective study of 162 cats (1996-2013). *J Vet Cardiol* 2015;17
341 Suppl 1:S215-9.
- 342 [10] Tidholm A. Retrospective study of congenital heart defects in 151 dogs. *J*
343 *Small Anim Pract* 1997;38:94-8.
- 344 [11] Oliveira P, Domenech O, Silva J, Vannini S, Bussadori R, Bussadori C.
345 Retrospective review of congenital heart disease in 976 dogs. *J Vet Intern Med*
346 2011;25:477-83.
- 347 [12] Koo ST, LeBlanc NL, Scollan KF, Sisson DD. Complete transposition of the
348 great arteries with double outlet right ventricle in a dog. *J Vet Cardiol* 2016;18:179-
349 86.
- 350 [13] Vos JH, van der Linde-Sipman JS, Stokhof AA. Double outlet left ventricle in a
351 dog. *Vet Pathol.* 1984;21:174-7.
- 352 [14] Jeraj K, Ogburn PN, Jessen CA, Miller JD, Schenk MP. Double outlet right
353 ventricle in a cat. *J Am Vet Med Assoc* 1978;173:1356-60.
- 354 [15] Abduch MC, Tonini PL, de Oliveira Domingos Barbusci L, de Oliveira SM, de
355 Freitas RR, Aiello VD. Double-outlet right ventricle associated with discordant
356 atrioventricular connection and dextrocardia in a cat. *J Small Anim Pract*
357 2003;44:374-7.
- 358 [16] Kohnken R, Schober K, Godman J, Gardner A, Jenkins T, Schroeder E, Baker
359 P, Dunbar L. Double outlet right ventricle with subpulmonary ventricular septal defect

360 (Taussig-Bing anomaly) and other complex congenital cardiac malformations in an
361 American Quarter Horse foal. *J Vet Cardiol* 2018;20:64-72.

362 [17] Chaffin MK, Miller MW, Morris EL. Double outlet right ventricle and other
363 associated congenital cardiac anomalies in an American miniature horse foal. *Equine*
364 *Vet J* 1992;24:402-6.

365 [18] Stieger-Vanegas SM, Scollan KF, Meadows L, Sisson D, Schlipf J, Riebold T,
366 Löhr CV. Cardiac-gated computed tomography angiography in three alpacas with
367 complex congenital heart disease. *J Vet Cardiol* 2016;18:88-98.

368 [19] Wilson RB, Cave JS, Horn JB, Kasselberg AG. Double outlet right ventricle in
369 a calf. *Can J Comp Med* 1985;49:115-6.

370 [20] Prosek R, Oyama MA, Church WM, Nagy DW, Sisson DD. Double-outlet right
371 ventricle in an Angus calf. *J Vet Intern Med* 2005;19:262-7.

372 [21] Witham AC. Double-outlet right ventricle: a partial transposition complex. *Am*
373 *Heart J* 1957;53:928-39.

374 [22] Tchervenkov CI, Walters HL 3rd, Chu VF. Congenital Heart Surgery
375 Nomenclature and Database Project: double outlet left ventricle. *Ann Thorac Surg*
376 2000;69(4 Suppl):S264-9.

377 [23] Mahle WT, Martinez R, Silverman N, Cohen MS, Anderson RH. Anatomy,
378 echocardiography, and surgical approach to double outlet right ventricle. *Cardiol*
379 *Young* 2008;18 Suppl 3:39-51.

380 [24] Pang KJ, Meng H, Hu SS, Wang H, Hsi D, Hua ZD, Pan XB, Li SJ.
381 Echocardiographic Classification and Surgical Approaches to Double-Outlet Right
382 Ventricle for Great Arteries Arising Almost Exclusively from the Right Ventricle. *Tex*
383 *Heart Inst J* 2017;44:245-51.

384 [25] Shi K, Yang ZG, Chen J, Zhang G, Xu HY, Guo YK. Assessment of double
385 outlet right ventricle associated with multiple malformations in pediatric patients using
386 retrospective ecg-gated dual-source computed tomography. PLoS One
387 2015;10:e0130987.

388 **Footnotes**

389 ^d Vivid 7, Vivid E9; General Electric Medical System, Waukesha, WI, USA.

390 ^e Brilliance 64-slice CT scanner, Philips Medical Systems, Cleveland, OH, USA.

391

392 ^f 3mensio, PIE Medical Imaging, Maastricht, The Netherlands.

393

394 ^g Prilactone, CEVA, Libourne, France.

395 ^h Agepi Oméga 3, MP Labo, Grasse, France.

396 ⁱ Nelio, CEVA, Libourne, France.

397 ^j Dimazon, Intervet, Beaucouze, France.

398 **Figure legends**

399 **Figure 1: Representative color-flow Doppler (A, B) and three-dimensional**
400 **retrospective ECG-gated (phase 30%) computed tomography (CT)**
401 **reconstruction of the heart and great vessels (C and D) from a 17-month-old**
402 **Poodle dog with double outlet right ventricle (Case 1).**

403 **A and B** - Color-flow Doppler images obtained from the right parasternal 5-chamber
404 view confirming a left-to-right shunt through the ventricular septal defect during the
405 early systolic phase (A) and the presence of right ventricle-aortic flow during the
406 whole systolic phase (B)

407 **C** - This CT image confirms a large ventricular septal defect (VSD) with the aorta
408 exiting from the hypertrophied right ventricle.

409 **D** – Note on this CT image the presence of an aberrant coronary artery exiting from
410 the pulmonary trunk.

411 Ao: aorta; LA: left atrium; LV: left ventricle; RV: right ventricle.

412

413 **Figure 2: Images from a 1.5-year-old Yorkshire Terrier dog diagnosed with**
414 **double outlet right ventricle (Case 2).**

415 **A and B** - Two-dimensional (A) and color-flow-Doppler mode (B) images respectively
416 obtained from the right parasternal transaortic short-axis view and a right parasternal
417 long-axis view, showing that both arteries arise from the right ventricle. Other
418 abnormalities (B) include a turbulent left-to-right shunt through a small-sized defect
419 within the muscular part of the interventricular septum and a subaortic stenosis (white
420 arrows). The connection between the right ventricle and the aorta is show by an
421 asterisk in both figures.

422 **C** - Necropsy examination (after oblique incision of the right ventricle) confirming that

423 the aorta and the pulmonary trunk both emerge from the right ventricle. Note also the
424 small muscular non-committed ventricular septal defect (arrow).

425 **D** - Histopathological examination showing a major remodeling of the pulmonary
426 arteries with marked obliterative muscular hypertrophy (arrow) and intimal thickening.
427 These plexiform lesions are consistent with pulmonary arteriopathy due to severe
428 pulmonary arterial hypertension. Hematoxylin, eosin and saffron stain (Anatomical
429 Pathology department, BioPôle Alfort, Ecole Nationale Vétérinaire d'Alfort)

430 Ao: aorta; LA: left atrium; LVPW: left ventricular posterior wall; PT: pulmonary trunk;
431 RA: right atrium; RV: right ventricle; RVW: right ventricular wall; VSD: ventricular
432 septal defect.

433

434 **Figure 3: Two-dimensional (A) and color-flow-Doppler mode (B) images**
435 **recorded in a 4-month-old male Samoyed dog diagnosed with double outlet**
436 **right ventricle (Case 3), respectively from the right parasternal 5-chamber view**
437 **and the right parasternal transaortic short-axis view.** Both images confirm that
438 the aorta arises from the right ventricle. Figure 3A additionally shows a large
439 ventricular septal defect (arrow) and Figure 3B a non-aliased ascending flow within
440 the pulmonary trunk (arrow) owing to the presence of a patent ductus arteriosus.

441 Ao: aorta; LA: left atrium; LV: left ventricle; PT: pulmonary trunk; RV: right ventricle.

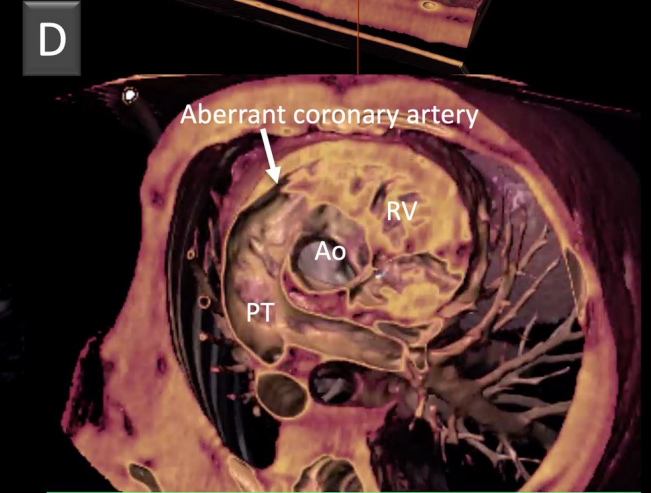
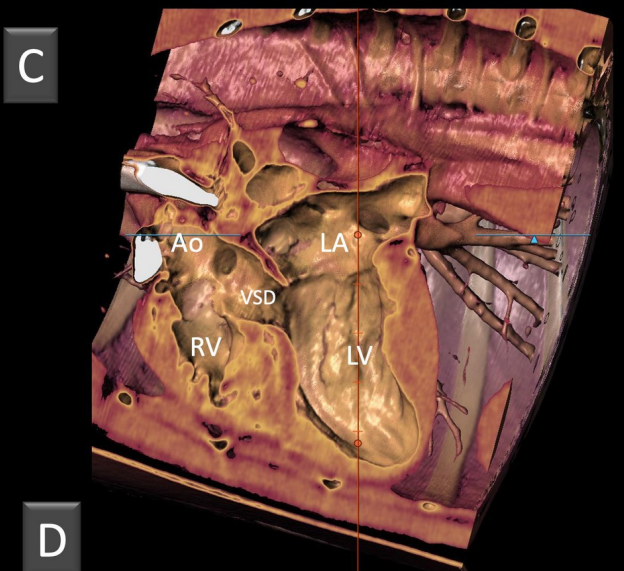
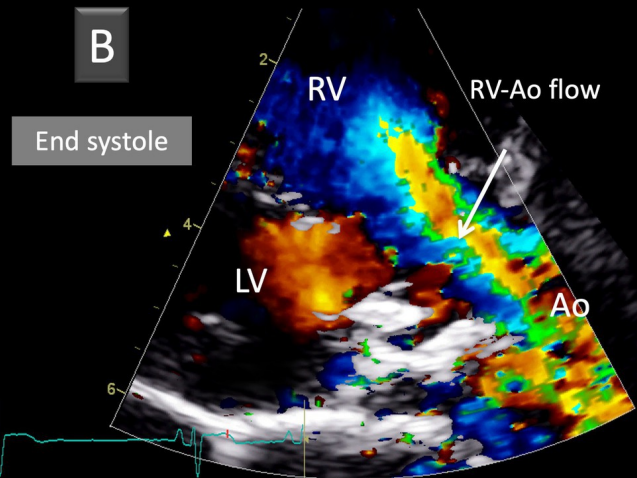
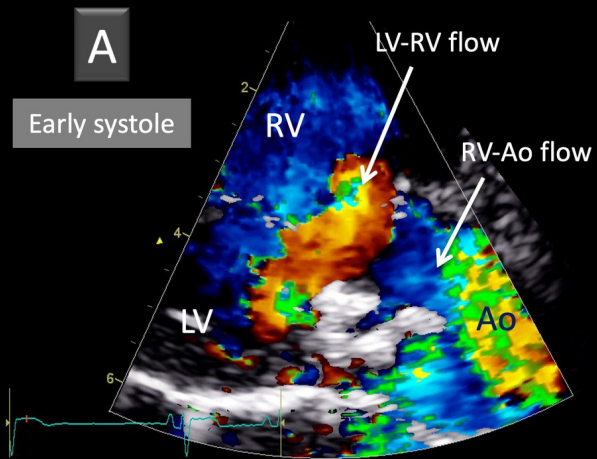
442

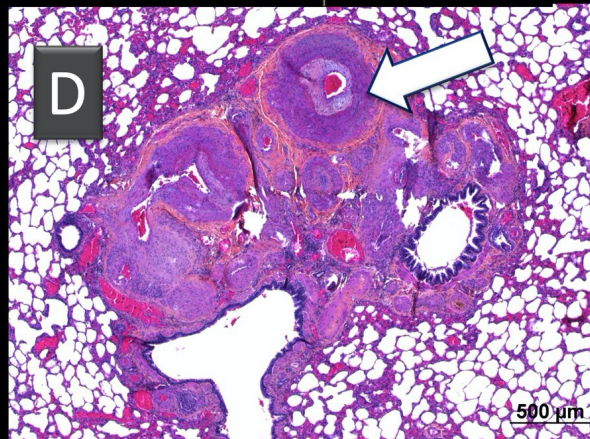
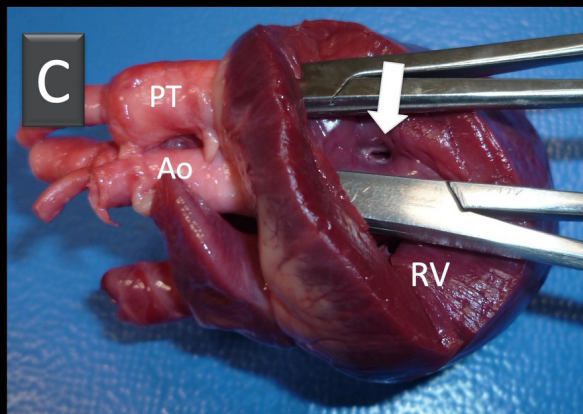
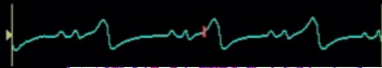
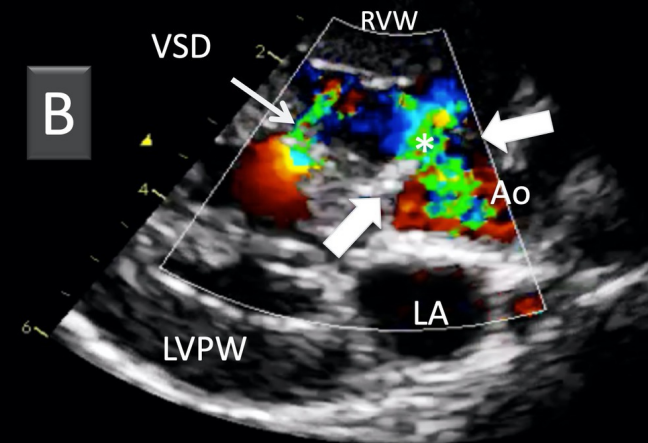
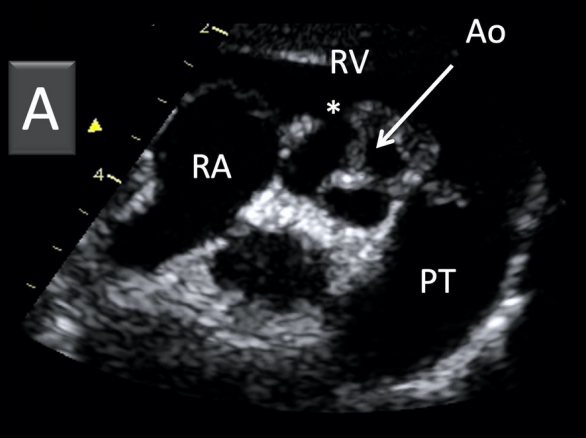
443 **Figure 4: Two-dimensional (A) and color-flow Doppler mode (B and C) systolic**
444 **images recorded in a 6-month-old female cat diagnosed with double outlet**
445 **right ventricle (Case 5), obtained from a left cranial parasternal short-axis view**
446 **(A) and two right parasternal long-axis views (B and C).** Note the abnormal right
447 lateral position of the aorta (A and B) and the systolic left-to-right shunt through a

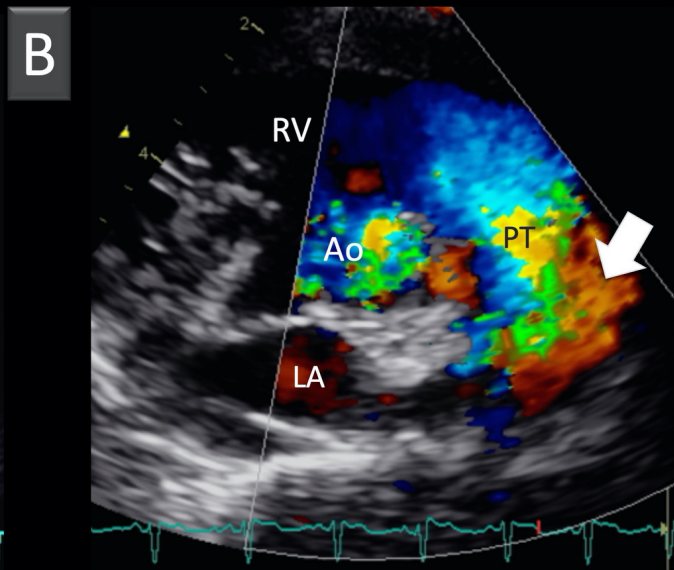
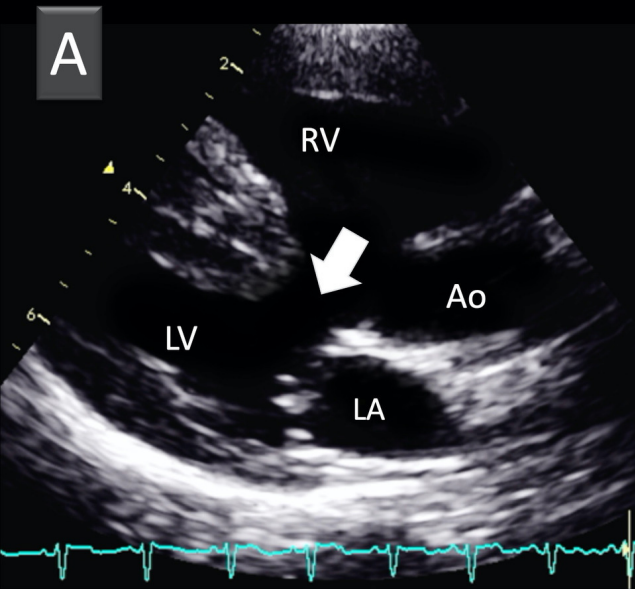
448 large defect within the interventricular septum (C). The larger diameter of the
449 pulmonary trunk, as compared with that of the aorta, may be due to the increased
450 flow coming from the ventricular septal defect.

451 Ao: aorta; LA: left atrium; LV: left ventricle; PT: pulmonary trunk; RA: right atrium; RV:
452 right ventricle; RVW: right ventricular wall.

453







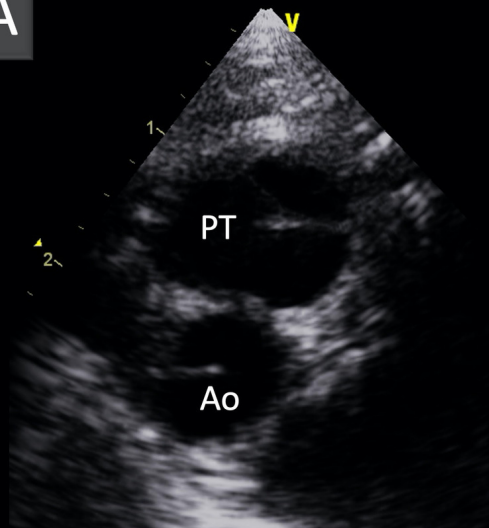
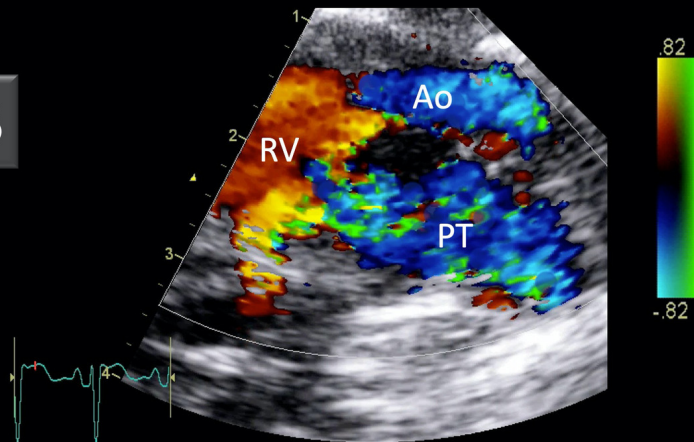
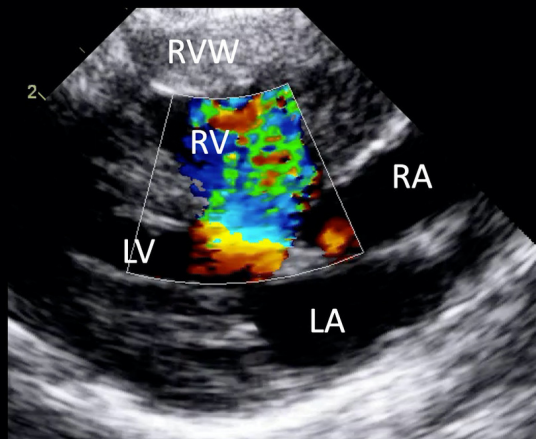
A**B****C**

Table 1: Video captions

Video number	Description
Video 1	Contrast-enhanced retrospective ECG-gated multidetector computed tomography scan with two- and three-dimensional orthogonal views showing the large ventricular septal defect and the aorta emerging from the right ventricle. The aberrant coronary artery exiting from the pulmonary trunk is also seen in the two movies on the left.
Video 2	Contrast-enhanced retrospective ECG-gated multidetector computed tomography scan with two- and three-dimensional orthogonal views showing the aorta and the pulmonary trunk both emerging from the right ventricle, with an aberrant coronary artery from the pulmonary trunk. Note the absence of left ventricular outflow track.
Video 3	Contrast-enhanced retrospective ECG-gated multidetector computed tomography scan: volume rendering video.